DOI: 10.1002/chem.200800666

Spontaneous Resolution of Chiral Polyoxometalate-Based Compounds Consisting of 3D Chiral Inorganic Skeletons Assembled from Different Helical Units

Ya-Qian Lan, Shun-Li Li, Xin-Long Wang, Kui-Zhan Shao, Dong-Ying Du, Zhong-Min Su,* and En-Bo Wang*[a]

Abstract: Four enantiomerically pure 3D chiral POM-based compounds, $[Ni_2(bbi)_2(H_2O)_4V_4O_{12}]\cdot 2H_2O$ (**1a** and **1b**) and $[Co(bbi)(H_2O)V_2O_6]$ (**2a** and **2b**) (bbi = 1,1′-(1,4-butanediyl)bisimidazole) based on the achiral ligand, different vanadate chains, and different metal centers have been synthesized by hydrothermal methods. Single-crystal X-ray diffraction analyses revealed that **1a** and **1b**, and **2a** and **2b**, respectively, are enantiomers. In **1a** and **1b** two kinds of vanadate chains with different screw axes link Ni cations to generate 3D chiral inorganic skeletons, which are connected by the achiral bbi ligands to form complicated 3D 3,4-connected chiral self-penetrating frameworks with $(7^2\cdot 8)(7^2\cdot 8^2\cdot 9^2)(7^3\cdot 8^2\cdot 10)$ topology. They represent the first examples of chiral self-penetrating frameworks known for polyoxometalate (POM) systems. Contrary to **1a** and **1b**, in **2a** and **2b** the vanadate chains link Co^{II} cations to generate 3D chiral inorganic skeletons, which are assembled from two kinds of heterometallic helical units of opposite chirality along the *c* axes. The chiral inorganic skeletons are connected by bbi to form 3D 3,4-connected chiral POM-based frameworks with $(6^2\cdot 8)_2(6^2\cdot 8^2\cdot 10^2)$ topology. It is believed that the asymmetrical coordination modes of the metal cations in **1a**–**2b** generate the initial chiral centers, and that the formation of the various helical units and the hydrogen bond interactions are responsible for preservation of the chirality and spontaneous resolution when the chirality is extended into the homochiral 3D-networks. This is the first known report of chiral POM-based compounds consisting of 3D chiral inorganic skeletons being obtained by spontaneous resolution upon crystallization in the absence of any chiral source, which may provide a rational strategy for synthesis of chiral POM-based compounds by using achiral ligands and POM helical units.

Keywords: chain structures · chiral resolution · helical structures · polyoxometalates · synthetic methods

Introduction

Chiral inorganic-organic materials have received much attention not only because of their potential applications, but also owing to their intriguing variety of architectures and topologies.[1–3] Polyoxometalates (POMs),[4] a unique class of metal oxide clusters, have many properties that make them attractive for applications in medicine, biology, magnetism, materials science, and catalysis.[5] Assembly of chiral POM-based compounds, which may incorporate functionality from both POMs and chiral materials, is currently an active research field.[6] In recent years, a few chiral POM-based compounds have been observed, most of which are discrete or low-dimensional structures.[7] The rational synthesis of chiral high-dimensional frameworks constructed from POM units is still a great challenge, however.

Two main approaches have been developed for the formation of chiral POM-based frameworks. The first method is based on the use of chiral species (chiral organic linkers or chiral metal complexes) as structure-directing agents; a few prominent results based on this approach have been report-

[a] Dr. Y.-Q. Lan, Dr. S.-L. Li, Dr. X.-L. Wang, Dr. K.-Z. Shao, D.-Y. Du, Prof. Z.-M. Su, Prof. E.-B. Wang
Institute of Functional Material Chemistry
Key Laboratory of Polyoxometalate Science of Ministry of Education, Faculty of Chemistry
Northeast Normal University
Changchun 130024 (People's Republic of China)
Fax: (+86) 431 85099108
E-mail: zmsu@nenu.edu.cn
wangenbo@public.cc.jl.cn

Supporting information for this article, including additional figures and TGA, XRPD, UV/Vis, and EIMS, is available on the WWW under http://dx.doi.org/10.1002/chem.200800666.

ed recently thanks to the work of Pope, Hill, Yamase, and Kortz.[8] The second approach is based on the use of achiral ligands with spontaneous resolution without any chiral auxiliaries, which yields a conglomerate.[9] Statistically, between 5 and 10% of all racemates form conglomerate crystals,[10] indicating that heterochiral interactions are prevalent and more facile than homochiral interactions in the formation of crystalline racemates.[11] To date, only two chiral POM-based compounds have been obtained by spontaneous resolution upon crystallization.[12] One was constructed from hafnium-substituted polyoxometalate $[Hf(PW_{11}O_{39})_2]^{10-}$ by Hill,[12a] and the other, the first example of an enantiomerically pure 3D POM-based compound with achiral ligands, the $[V_{10}O_{26}]^{4-}$ polyoxoanion, and mixed-valence $Cu^{I/II}$, was synthesized by our group.[12b]

One of the principal challenges in the construction of inorganic–organic hybrid materials is the control of the dimensionality by the inorganic connectivity.[13] Inorganic components are isolated by metal cations or polyoxoanion clusters in the majority of POM-based compounds, and only a very limited number of examples of 3D inorganic connectivity are known.[14,15] Design of the construction of chiral POM-based compounds is more difficult when inorganic connectivity with spontaneous resolution is used without any chiral auxiliary. Such compounds have not been observed to date, and therefore the search for suitable achiral organic molecules, metal cations, and POM building units to construct them is one of the most challenging issues in synthetic chemistry and materials science.

In accord with the literature,[16] we chose the flexible ligand 1,1′-(1,4-butanediyl)bisimidazole (bbi) as the achiral ligand, a vanadate chain as the polyoxoanion, and different metal ions to synthesize chiral POM-based 3D frameworks based on the following considerations: i) many chiral compounds have been constructed on the basis of helical topology,[17] and helical units can be formed by vanadate chains by changing the reaction pH;[18] ii) in comparison with isolated metal oxide clusters, 1D vanadate chains have great advantages for constructing high-dimensional inorganic connectivity frameworks; iii) conformational changes of flexible bbi ligands often lead to the lack of a center of symmetry, with the benefit that they then form chiral compounds. As accurate prediction of the final structures is impossible, we have tried different synthetic conditions and performed many experiments. Fortunately, $[Ni_2(bbi)_2(H_2O)_4V_4O_{12}]\cdot 2H_2O$ (**1a** and **1b**) and $[Co(bbi)(H_2O)V_2O_6]$ (**2a** and **2b**) are isolated successfully by hydrothermal methods and separated manually (Supporting Information, Figure S1). Single-crystal X-ray diffraction analyses reveal that the structures of compounds **1a** and **1b**, and **2a** and **2b**, respectively, are enantiomers. Their unit cell dimensions, volumes, related bond lengths, and angles are only slightly different. To the best of our knowledge, it is the first time that chiral POM-based compounds consisting of 3D chiral inorganic skeletons have been obtained by spontaneous resolution upon crystallization in the absence of any chiral source, which may demonstrate a rational strategy for synthesis of these compounds by using achiral ligands and POM helical units. In addition, **1a–2b** have been characterized further by elemental analyses, IR, UV/Vis, and CD spectra, and thermogravimetric analyses (TGAs).

Results and Discussion

Structures: Single-crystal X-ray diffraction analyses show that **1a** crystallizes in the chiral space group $P4_12_12$, and **1b** in the space group $P4_32_12$. They are made up of one kind of Ni cation, two kinds of anions ($(VO_3)^-$ and $(V_2O_6)^{2-}$, respectively), one kind of bbi ligand, and water molecules (Figure 1). The Ni center exhibits a distorted octahedral geometry and is surrounded by two nitrogen atoms from different bbi ligands, two oxygen atoms from different anions ($(VO_3)^-$ and $(V_2O_6)^{2-}$, respectively), and two oxygen atoms from two water molecules. The bbi ligand exhibits TTG (T = *trans*; G = *gauche*) conformation (Supporting Information, Figure S2) and acts as a bidentate ligand coordinated to two Ni cations. The dihedral angle between the two imidazole rings is 89.8° for **1a** and 90.3° for **1b**. All the V cations are four-coordinated by four oxygen atoms in tetrahedral geometries. Here, the VO_4 tetrahedra of the V1 cations are linked to each other in corner-sharing modes to generate a $[(VO_3)^-]_8$ helical chain with a four-fold screw axis (a right-handed helix in **1a** with a 4_1 helical axis; a left-handed helix in **1b** with a 4_3 helical axis; the 4_1 and 4_3 axes are mirror images of each other) (Figure 2) along the *c* axis, and those of the V2 and V3 cations are linked each other in corner-sharing modes to generate a $[(V_2O_6)^{2-}]_8$ helical chain, with a two-fold screw axis along the *c* axis (a left-handed helix in **1a**; a right-handed helix in **1b**). It is interesting that the two kinds of helical chains are connected by Ni cations to form a 3D chiral inorganic skeleton, which is a 3,4-connected framework with $(7\cdot8^2)2(7\cdot8^5)$ topology (Supporting Information, Figure S3). These inorganic skeletons are mirror images in **1a** and **1b** (Figure 3). The bbi ligands link the Ni

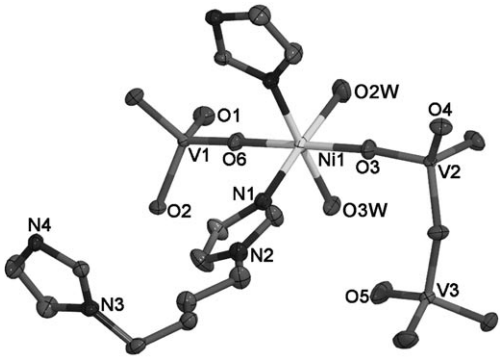

Figure 1. ORTEP diagram showing the coordination environments for the Ni atom in **1a** with thermal ellipsoids at the 30% probability displacement. Only some of the atoms are labeled, and all the hydrogen atoms and lattice water molecules are omitted for clarity.

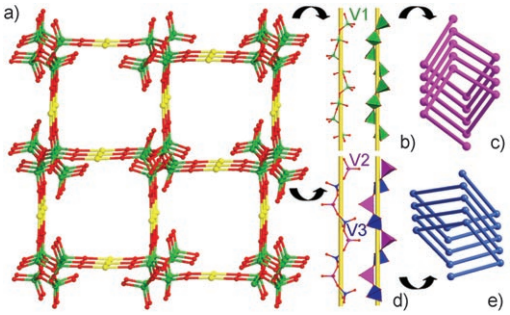

Figure 2. a) Ball-and-stick representations of the 3D chiral inorganic skeleton in **1a**. b) Ball-and-stick and polyhedral representations of the $[(VO_3)^-]_8$ helical chain (a right-handed helix in **1a** with a 4_1 helical axis). c) Schematic representation of the $[(VO_3)^-]_8$ helical chain. d) Ball-and-stick and polyhedral representations of the $[(V_2O_6)^{2-}]_8$ helical chain (a left-handed helix in **1a** with a 2_1 helical axis). e) Schematic representation of the $[(V_2O_6)^{2-}]_8$ helical chain.

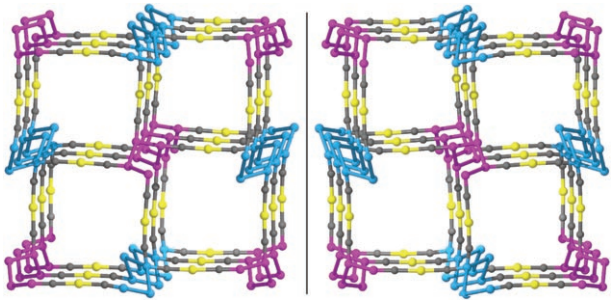

Figure 3. Schematic representations of mirror images of 3D chiral inorganic skeletons in **1a** (left) and **1b** (right).

cations to generate chains, which interweave like the "warp" and "weft" along the *a* and *b* axes to form a molecular fabric structure (Supporting Information, Figure S4).[19] The inorganic skeleton and the molecular fabric structure described above are fused by sharing Ni centers to form a complicated 3D POM-based chiral framework. In this net, two crystalligraphically related rings with composition -Ni-bbi-VO_4-Ni-V_4O_{13}- are catenated with each other to give a self-penetrating (self-catenation or polyknotting) 3D structure (Figure 4). Self-penetrating structures defined by Ciani and coworkers are single nets that have the peculiarity that the smallest topological rings are catenated by other rings belonging to the same network.[20] A few coordination compounds exhibiting self-penetrating network architectures have been reported.[21] However, the 3D chiral POM-based self-penetrating framework has not been observed. From the topological viewpoint, the nets of **1a** and **1b** can be considered as 3D 3,4-connected frameworks based on each VO_4 (V1) tetrahedron as a three-connected node, each VO_4 (V2) tetrahedron as a four-connected node, the Ni cation as a four-connected node, and the bbi ligand and VO_4 (V3) tetrahedron as linkers (Supporting Information, Figure S5). The Schläfli symbol is $(7^2{\cdot}8)(7^2{\cdot}8^2{\cdot}9^2)(7^3{\cdot}8^2{\cdot}10)$ (Figure 4c).

The results mentioned above encouraged us to expand our studies to the Co^{II} analogues. The naive expectation was

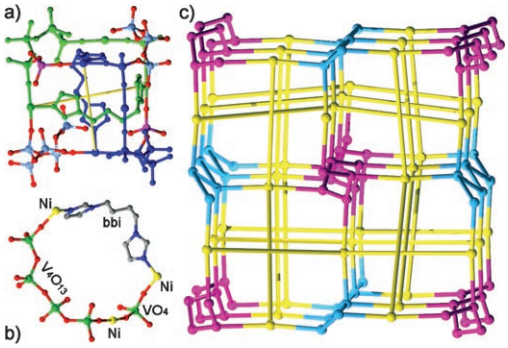

Figure 4. a) Ball-and-stick representations of the self-penetrating framework in **1a**. b) One ring with the composition -Ni-bbi-VO_4-Ni-V_4O_{13}- in the self-penetrating framework. c) Schematic representation of the (3,4)-connected framework with $(7^2{\cdot}8)(7^2{\cdot}8^2{\cdot}9^2)(7^3{\cdot}8^2{\cdot}10)$ topology.

that the structural chemistry would be analogous to that of Ni^{II}. In fact, the results are largely unexpected. Compounds **2a** and **2b** crystallize in the chiral space group $P2_12_12$. X-ray diffraction analyses reveal that there is one kind of Co cation, one kind of $(V_2O_6)^{2-}$ anion, one kind of bbi ligand, and one water molecule in the crystallographically unique unit (Figure 5). The Co center is in a distorted square pyra-

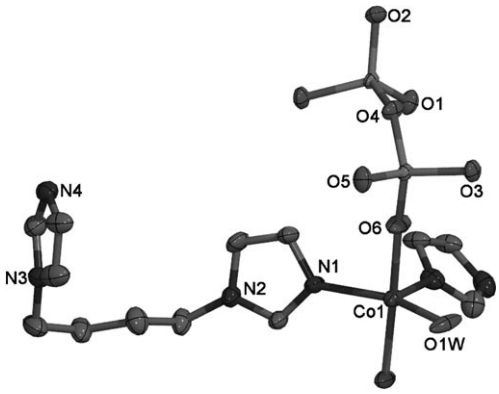

Figure 5. ORTEP diagram showing the coordination environments for the Co atom in **2a** with thermal ellipsoids at the 30% probability displacement. Only some of the atoms are labeled, and all the hydrogen atoms are omitted for clarity.

midal geometry that is coordinated by two nitrogen atoms from different bbi ligands, two oxygen atoms from different $(V_2O_6)^{2-}$ anions, and one water molecule. The bbi ligand exhibits a TTG conformation (Supporting Information, Figure S2) and acts as a bidentate ligand coordinated to two Co cations. The dihedral angle between the two imidazole rings is 55.4° for **2a** and 58.2° for **2b**. All V cations are four-coordinated by four oxygen atoms in tetrahedral geometries. These tetrahedra are linked each other in a corner-sharing mode to generate a $[(V_2O_6)^{2-}]_8$ chain along the *a* axis. Co cations connect $[(V_2O_6)^{2-}]_8$ chains to form a 3D chiral inorganic skeleton with chiral (10,3)-a topology (Supporting Information, Figure S6). Two kinds of heterometallic helical units (**I** and **II**) exist with opposite helicity along the crystal-

lographic *c* axis. The helical unit **I** is made up of a -Co1-V1-V2-Co1- chain (a right-handed helix in **2a** and a left-handed helix in **2b**, with 2_1 helical axes). The helical unit **II** is made up of a -Co1-V1-V2-V1-V2-Co1- chain (a left-handed helix in **2a** and a right-handed helix in **2b** with 2_1 helical axes) (Figure 6). Thus there are inorganic skeletons of opposite

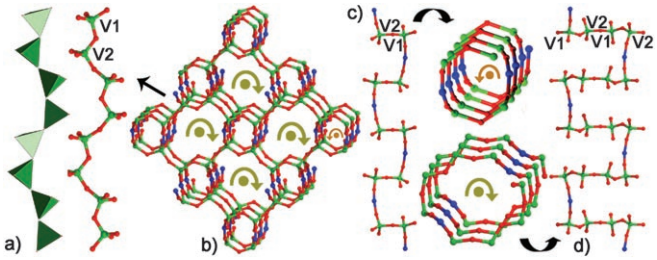

Figure 6. a) Ball-and-stick and polyhedral representations of the $[(V_2O_6)^{2-}]_8$ chain in **2a**. b) Ball-and-stick representations of the 3D chiral inorganic skeleton in **2a**. c) Schematic representation of the heterometallic helical unit **I** (a right-handed helix in **2a** with a 2_1 helical axis). d) Schematic representation of the heterometallic helical unit **II** (a left-handed helix in **2a** with a 2_1 helical axis). (The handedness of some helices is illustrated as arrows, and the center dot defines the direction as into the page)

chirality in the **2a** and **2b** frameworks (Figure 7). The bbi ligands link the Co cations to form a zigzag chain which adorns the larger helical channel of the above 3D inorganic skeleton (Figure 8a). The whole structures of **2a** and **2b** can be considered as 3,4-connected chiral POM-based frameworks based on the VO_4 (V1 and V2) tetrahedra as two kinds of three-connected nodes, the Co cation as a four-connected node, and bbi ligands as linkers (Supporting Information, Figure S7). The Schläfli symbol denotes the $(6^2{\cdot}8)_2(6^2{\cdot}8^2{\cdot}10^2)$ topology (Figure 8b).

In this case, compounds **1** and **2** are both conglomerates. They have been obtained by spontaneous resolution upon crystallization in the absence of any chiral source based on 3D chiral inorganic skeletons. They are mechanical and racemic mixtures of chiral crystals, in which each crystal is enantiopure and crystallizes in a chiral space group. If we can separate these racemic mixtures manually to obtain

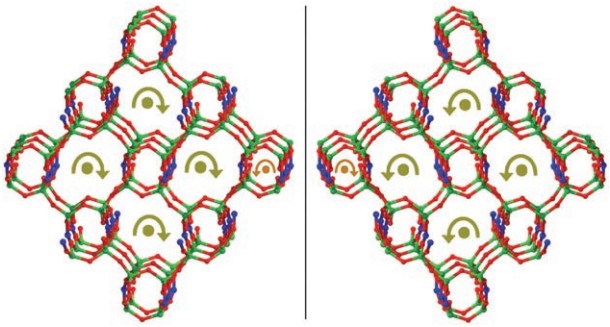

Figure 7. Schematic representations of mirror images of 3D chiral inorganic skeletons in compounds **2a** (left) and **2b** (right). (The handedness of some helices is illustrated as arrows, and the center dot defines the direction as inside of the page)

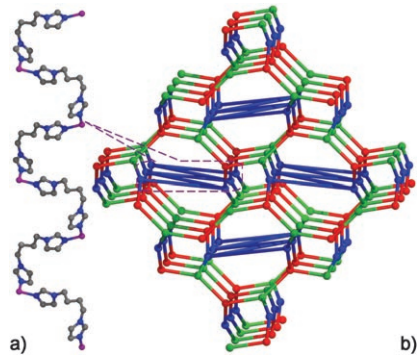

Figure 8. a) Ball-and-stick representations of the zigzag chain consisting of bbi ligands and Co cations in compound **2a**. b) Schematic representation of the (3,4)-connected framework with $(6^2{\cdot}8)_2(6^2{\cdot}8^2{\cdot}10^2)$ topology.

enantiopure compositions, it is beneficial to exploit the chiral properties of these species. Fortunately, two pairs of enantiomers (**1a** and **1b**, and **2a** and **2b**, respectively) can be separated manually by using the polarized light microscope (Supporting Information, Figure S1).

Spontaneous resolution, known as the segregation of enantiomers upon crystallization, was discovered as early as 1846 by Louis Pasteur,[22] and it is still a rare phenomenon that cannot be predicted a priori because the laws of physics determining the processes are not yet fully understood.[23] For compounds **1a**–**2b**, we investigated methods of generating initial chiral units without a chiral auxiliary, transferring the chiral units into homochiral structures of higher dimensionalities, and inducing spontaneous resolution. Offering further insight into the nature of these intricate architectures, we found that the Ni cations are coordinated to six different groups, namely two different VO_4 (V1 and V2) tetrahedra, two different bbi ligands, and two water molecules (O2W and O3W), via covalent linkages in **1a** and **1b**. In **2a** and **2b**, Co cations are coordinated to five different groups: two different VO_4 (V1 and V2) tetrahedra, two different bbi ligands, and one water molecule (O1W) (Figure 9). The Ni and Co cations are in asymmetrical coordination modes without mirror or inversion symmetry, and are considered as the initial chiral centers. Two kinds of vanadate helical chains with different screw axes link the Ni cations, and the chiral information may be transferred to the framework by helical units with two- or four-fold rotation, which leads to the chiral inorganic skeletons in compounds **1a** and **1b**. They differ from compounds **1a** and **1b** in that the chiral

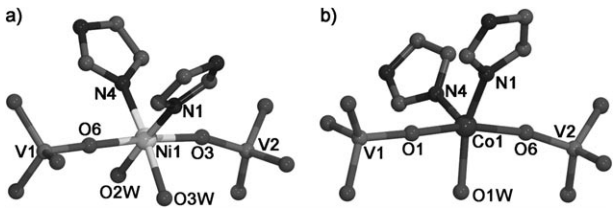

Figure 9. Ball-and-stick representations of the asymmetrical coordination modes for a) the Ni cations and b) the Co cations.

centers are connected by $(V_2O_7)^{4-}$ anions to give heterometallic helical chains, which are related by the two-fold screw axis and hence have the same chirality as the 3D skeletons in compounds **2a** and **2b**. In addition, hydrogen bonds play an important role in formation of the ultimate structures. As both **1a** and **1b** have the same hydrogen bond interactions, only that of **1a** is described in detail herein. As shown in the Supporting Information, Figure S8 and Table S1, one lattice water molecule (O1W) and coordinated water molecule (O3W) in **1a** form a dimer with an OW···OW distance of 2.729(3) Å, while such distances in regular ice, liquid water, and water vapor are 2.74, 2.85, and 2.98 Å, respectively.[24] The water molecules O1W and O2W donate H bonds to two oxygen atoms from different $[(VO_3)^-]_8$ and $[(V_2O_6)^{2-}]_8$ chains (O1#7 and O5#8 for O1W, and O1#1 and O5#2 for O2W), respectively. Similar hydrogen bonding interactions exist in **2a** and **2b**. Figure S9 (Supporting Information) shows hydrogen bonds in **2a**. The coordinated water molecule (O1W) donates two hydrogen bonds to two oxygen atoms (O2 and O5#3) from two adjacent $[(V_2O_6)^{2-}]_8$ chains. These hydrogen bonding interactions link chiral centers and two different helical chains in **1a** and **1b**, and two adjacent chains $[(V_2O_6)^{2-}]_8$ in **2a** and **2b**, respectively, which take part in transferring chiral information and further stabilize the 3D chiral inorganic frameworks. Clearly, the asymmetrical coordination modes of the metal cations generate the initial chiral centers, and the formation of the various helical units and the hydrogen bond interactions are expected to be responsible for the chirality preservation and spontaneous resolution when the chirality is extended into the homochiral 3D networks. To the best of our knowledge, it is the first time that chiral POM-based compounds consisting of 3D chiral inorganic skeletons have been obtained by spontaneous resolution upon crystallization in the absence of any chiral source, which may provide a rational strategy for synthesis of chiral POM-based compounds by using achiral ligands and POM helical units.

To characterize the compounds more fully in terms of thermal stability, we have examined compounds **1a** and **2a** using thermal gravimetric analysis (TGA) (Supporting Information, Figure S10). The TG curve of compound **1a** shows a weight loss of 10.6% from room temperature to 257°C, corresponding to the release of six lattice and coordinated water molecules (calculated loss 10.8%). Decomposition of the anhydrous composition begins at 365°C and ends above 546°C. The 38.5% weight loss corresponds to the loss of organic components (calculated loss 38.0%). The remaining weight (50.9%) corresponds to the percentage (51.2%) of Ni, V, and O components, indicating that the final product is possibly the mixture of NiO and V_2O_5. The TG curve of **2a** shows a weight loss of 4.0% from room temperature to 152°C, corresponding to the release of one coordinated water molecule (calculated loss 3.9%). The anhydrous composition begins to decompose at 320°C and ends above 710°C. The 40.5% weight loss corresponds to the loss of organic components (calculated loss 40.9%). The remaining weight of 55.5% corresponds to the percentage (55.2%) of Co, V, and O components, indicating that the final product is possibly the mixture of CoO and V_2O_5.

The X-ray powder diffraction patterns for **1a**–**2b** are presented in Figure S11 (Supporting Information). The diffraction peaks of both simulated and experimental patterns match well in key positions, thus indicating the phase purities of **1a**–**2b**.

Circular dichroism (CD) spectroscopy has emerged as a very useful technique in stereochemistry in recent years.[1c,25] To examine the chiroptical and stable activities of all the nantiopure compounds in the solution state, the CD spectra of **1a**–**2b** in DMSO have been investigated (Figure 10 and Supporting Information, Figure S12). The CD spectra of each pair of compounds **1a** and **1b**, and **2a** and **2b**, are mirror images of each other, indicating that the two pairs of compounds are the respective enantiomers. In the wavelength range $\lambda = 200$–300 nm, **1a** shows negative Cotton effects at $\lambda = 212$ and 244 nm and positive Cotton effects at $\lambda = 237$ and 253 nm, whereas **2a** shows a negative Cotton effect at $\lambda = 236$ nm and positive Cotton effects at $\lambda = 250$ and 259 nm. Compounds **1b** and **2b** show Cotton effects of the opposite signs to **1a** and **2a** at the same wavelengths. However, EIMS of **1a** and **2a** in DMSO show that they decompose to some small fragments (Supporting Information, Figure S13). The interesting CD spectral results indicate that these small fragments retain the chirality, which may suggest that there are stable interactions among small fragments in solution.

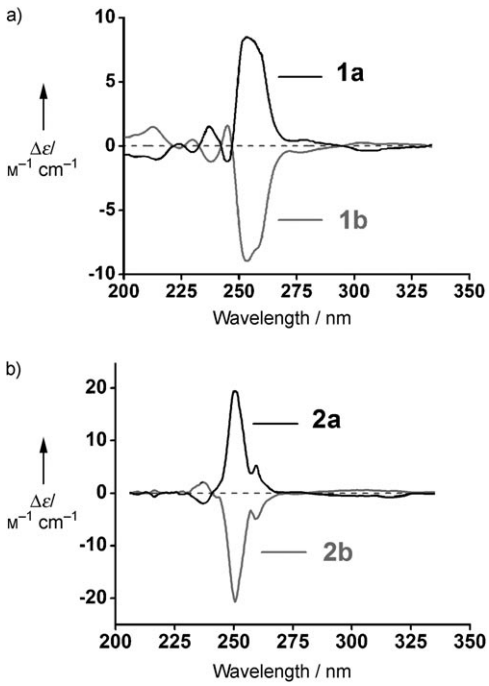

Figure 10. a) The CD spectra of **1a** and **1b** in DMSO (**1a**: $c = 5.0 \times 10^{-4}$ M and **1b**: $c = 5.2 \times 10^{-4}$ M). b) The CD spectra of **2a** and **2b** in DMSO (**2a**: $c = 6.0 \times 10^{-4}$ M and **2b**: $c = 6.1 \times 10^{-4}$ M).

Conclusion

In summary, we have prepared by hydrothermal methods and characterized four enantiomerically pure 3D chiral POM-based architectures based on an achiral ligand, different vanadate chains, and different metal centers without any chiral auxiliaries. These compounds consist of 3D chiral inorganic skeletons which are assembled from different helical units. In **1a** and **1b**, the 3D chiral inorganic skeletons are assembled from two kinds of helical vanadate chains with different screw axes. Compounds **2a** and **2b** differ from **1a** and **1b**: the vanadate chains link Co cations to generate 3D chiral inorganic skeletons, which are assembled from two kinds of heterometallic helical units with opposite chirality along the *c* axis. Compounds **1a** and **1b** represent the first examples of chiral self-penetrating frameworks of POM systems known at present. To the best of our knowledge, it is the first time that chiral POM-based compounds consisting of 3D chiral inorganic skeletons have been obtained by spontaneous resolution upon crystallization in the absence of any chiral source. The successful isolation of these species not only produces intriguing examples of enantiomerically pure architectures but may also provide a rational strategy for synthesis of chiral POM-based compounds by using achiral ligands and POM helical units.

Experimental Section

Materials and methods: All reagents and solvents for syntheses were purchased from commercial sources and used as received. The C, H, and N elemental analyses were conducted by using a Perkin–Elmer 240C elemental analyzer, and Ni, Co, and V were analyzed by using a Plasma-Spec (I) ICP (inductively coupled plasma) atomic emission spectrometer. The FTIR spectra were recorded from KBr pellets in the range $\tilde{\nu}=4000$–$400\,cm^{-1}$ by using a Mattson Alpha-Centauri spectrometer. The X-ray powder diffraction (XRPD) patterns were recorded by using a Siemens D5005 diffractometer with $Cu_{K\alpha}$ ($\lambda=1.5418$ Å) radiation. The UV/Vis spectra were recorded by using a Hitachi UV-3010 spectrophotometer. The CD spectra for the enantiomers were recorded by means of a Jasco J-810 spectropolarimeter. Mass spectra were collected by using a Bruker microTOF Q mass spectrometer in electrospray ionization (ESI) mode. Thermogravimetric analyses of the samples were performed by using a Perkin–Elmer TG-7 analyzer heated from room temperature to 800 °C under nitrogen at a rate of $10\,°C\,min^{-1}$.

Synthesis of $[Ni_2(bbi)_2(H_2O)_4V_4O_{12}]\cdot 2H_2O$ (1a and 1b): A mixture of NH_4VO_3 (0.117 g, 1 mmol), BBI (0.095 g, 0.5 mmol), $Ni(NO_3)_2\cdot 6H_2O$ (0.145 g, 0.5 mmol), and H_2O (10 mL) was adjusted to pH ≈ 4 and stirred for 1 h, and then transferred and sealed in a 25 mL Teflon-lined stainless steel container, which was heated at 150 °C for 72 h and then cooled to room temperature at a rate of $10\,°C\,h^{-1}$. Green crystals of **1** were collected in 52.1 % yield based on $Ni(NO_3)_2\cdot 6H_2O$. IR: $\tilde{\nu}=3924$ (m), 3897 (m), 3861 (s), 3845 (s), 3742 (s), 3679 (m), 3649 (w), 3115 (s), 1740 (w), 1678 (w), 1646 (m), 1563 (w), 1515 (s), 1455 (m), 1094 (w), 932 (s), 814 (s), 646 (s), 420 cm^{-1} (m); elemental analysis calcd (%) for $C_{20}H_{40}N_8O_{18}Ni_2V_4$ (1001.78): C 23.98, H 4.02, N 11.19, Ni 11.72, V 20.34; found: C 24.02, H 3.98, N 11.21, Ni 11.76, V 20.31.

Synthesis of $[Co(bbi)(H_2O)V_2O_6]$ (2a and 2b): A mixture of NH_4VO_3 (0.117 g, 1 mmol), BBI (0.095 g, 0.5 mmol), $Co(NO_3)_2\cdot 6H_2O$ (0.146 g, 0.5 mmol), and H_2O (10 mL) was adjusted to pH ≈ 2 and stirred for 1 h, and then transferred and sealed in a 25 mL Teflon-lined stainless steel container, which was heated at 150 °C for 72 h and then cooled to room temperature at a rate of $10\,°C\,h^{-1}$. Black crystals of **2** were collected in 48.6 % yield based on $Co(NO_3)_2\cdot 6H_2O$. IR: $\tilde{\nu}=3924$ (m), 3861 (m), 3742 (s), 3679 (m), 3649 (m), 3621 (m), 3108 (s), 1740 (w), 1693 (w), 1646 (w), 1515 (s), 1454 (w), 1398 (w), 1283 (w), 1234 (w), 1106 (m), 928 (s), 791 (s), 659 (s), 419 cm^{-1} (s); elemental analysis calcd (%) for $C_{10}H_{16}N_4O_7CoV_2$ (465.08): C 25.83, H 3.47, N 12.05, Co 12.67, V 21.91; found: C 25.80, H 3.51, N 12.8, Co 12.62, V 21.88.

Single-crystal structure analysis: Single-crystal X-ray diffraction data for **1a**, **1b**, **2a**, and **2b** were recorded by using a Bruker Apex CCD diffractometer with graphite-monochromated $Mo_{K\alpha}$ radiation ($\lambda=0.71073$ Å) at $T=293$ K. Absorption corrections were applied by using a multi-scan technique. All the structures were solved by the direct method of SHELXS-97[26] and refined by full-matrix least-squares techniques using the SHELXL-97 program[27] within WINGX.[28] For **1a**, **1b**, **2a**, and **2b**, all H atoms bonded to the organic ligands were positioned geometrically and refined as riding atoms, and the water H atoms were located on a difference Fourier map. The Flack parameters (0.001(10) for **1a**, 0.014(14) for **1b**, 0.013(17) for **2a**, and 0.03(3) for **2b**) indicate that the absolute configurations are correct. The detailed crystallographic data and structure refinement parameters are summarized in Table 1. CCDC 683857 (**1a**), CCDC 686858 (**1b**), CCDC 686859 (**2a**) and CCDC 683860 (**2b**) contain the supplementary crystallographic data for this paper. These data can be obtained free of charge from The Cambridge Crystallographic Data Centre via www.ccdc.cam.ac.uk/data_request/cif.

Table 1. Crystal data and structure refinements for **1a**, **1b**, **2a**, and **2b**

	1a	**1b**	**2a**	**2b**
formula	$C_{20}H_{40}N_8O_{18}Ni_2V_4$	$C_{20}H_{40}N_8O_{18}Ni_2V_4$	$C_{10}H_{16}N_4O_7CoV_2$	$C_{10}H_{16}N_4O_7CoV_2$
M_r	1001.78	1001.78	465.08	465.08
crystal system	tetragonal	tetragonal	orthorhombic	orthorhombic
space group	$P4_12_12$	$P4_32_12$	$P2_12_12$	$P2_12_12$
a [Å]	17.978(2)	17.983(3)	11.188(4)	11.192(7)
b [Å]	17.978(2)	17.983(5)	11.864(4)	11.952(8)
c [Å]	11.086(2)	11.083(5)	12.574(4)	12.538(8)
α [°]	90	90	90	90
β [°]	90	90	90	90
γ [°]	90	90	90	90
V [Å^3]	3583.1(9)	3584(2)	1669.0(10)	1677.2(19)
Z	4	4	4	4
ρ_{calcd} [g cm^{-3}]	1.857	1.857	1.851	1.851
$F(000)$	2032	2032	932	932
reflns collected/unique	22139/4418	22141/4454	10365/3985	8607/2991
R(int)	0.0321	0.0469	0.0270	0.0392
GOF on F^2	1.027	1.012	1.045	1.081
R_1[a] [$I>2\sigma(I)$]	0.0219	0.0315	0.0258	0.0349
wR_2[b]	0.0499	0.0612	0.0593	0.0732
largest residuals [e Å^{-3}]	0.246/−0.212	0.284/−0.349	0.296/−0.245	0.705/−0.469
Flack parameter	0.001(10)	0.014(14)	0.013(17)	0.03(3)

[a] $R_1=\Sigma||F_o|-|F_c||/\Sigma|F_o|$. [b] $wR_2=|\Sigma w(|F_o|^2\mathrm{MN}-|F_c|^2)|/\Sigma|w(F_o^2)^2|^{1/2}$.

Acknowledgement

We are thankful for financial support from the Program for Changjiang Scholars and Innovative Research Team in University, the National Natural Science Foundation of China (nos. 20573016 and 20703008), and the Science Foundation for Young Teachers of Northeast Normal University (no. 20070309).

[1] a) L. J. Prins, J. Huskens, F. D. Jong, P. Timmerman, *Nature* **1999**, *398*, 498–502; b) J. Chin, S. S. Lee, K. J. Lee, S. Park, D. H. Kim, *Nature* **1999**, *401*, 254–257.

[2] a) X. H. Bu, H. Liu, M. Du, L. Zhang, Y. M. Guo, M. Shionoya, J. Ribas, *Inorg. Chem.* **2002**, *41*, 1855–1861; b) X. L. Wang, C. Qin, E. B. Wang, L. Xu, Z. M. Su, C. W. Hu, *Angew. Chem.* **2004**, *116*, 5146–5150; *Angew. Chem. Int. Ed.* **2004**, *43*, 5036–5040; c) Y. Cui, H. L. Ngo, P. S. White, W. B. Lin, *Chem. Commun.* **2002**, 1666–1667.

[3] a) X. M. Chen, G. F. Liu, *Chem. Eur. J.* **2002**, *8*, 4811–4817; b) R. G. Xiong, X. Z. You, B. F. Abrahams, Z. L. Xue, C. M. Che, *Angew. Chem.* **2001**, *113*, 4554–4557; *Angew. Chem. Int. Ed.* **2001**, *40*, 4422–4425.

[4] a) M. T. Pope, *Heteropoly and Isopoly Oxometalates*, Springer, Berlin, **1983**; b) C. L. Hill, *Chem. Rev.* **1998**, *98*, 1–2; c) K. Fukaya, T. Yamase, *Angew. Chem.* **2003**, *115*, 678–682; *Angew. Chem. Int. Ed.* **2003**, *42*, 654–658; d) C. D. Wu, C. Z. Lu, H. H. Zhuang, J. S. Huang, *J. Am. Chem. Soc.* **2002**, *124*, 3836–3837; e) M. I. Khan, E. Yohannes, R. J. Doedens, *Angew. Chem.* **1999**, *111*, 1374–1376; *Angew. Chem. Int. Ed.* **1999**, *38*, 1292–1294; f) P. J. Hagrman, D. Hagrman, J. Zubieta, *Angew. Chem.* **1999**, *111*, 2798–2848; *Angew. Chem. Int. Ed.* **1999**, *38*, 2638–2684; g) E. Burkholder, J. Zubieta, *Chem. Commun.* **2001**, 2056–2057.

[5] a) A. Müller, S. Q. N. Shah, H. Bögge, M. Schmidtmann, *Nature* **1999**, *397*, 48–50; b) P. Kögerler, L. Cronin, *Angew. Chem.* **2005**, *117*, 866–868; *Angew. Chem. Int. Ed.* **2005**, *44*, 844–846; c) L. Xu, M. Lu, B. B. Xu, Y. G. Wei, Z. H. Peng, D. R. Powell, *Angew. Chem.* **2002**, *114*, 4303–4306; *Angew. Chem. Int. Ed.* **2002**, *41*, 4129–4132.

[6] a) A. Müller, F. Peters, M. T. Pope, D. Gatteschi, *Chem. Rev.* **1998**, *98*, 239–271; b) D. A. J. Judd, H. Nettles, N. Nevins, J. P. Snyder, D. C. Liotta, J. Tang, J. Ermolieff, R. F. Schinazi, C. L. Hill, *J. Am. Chem. Soc.* **2001**, *123*, 886–897.

[7] a) T. A. Sullens, R. A. Jensen, T. Y. Shvareva, T. E. Albrecht-Schmitt, *J. Am. Chem. Soc.* **2004**, *126*, 2676–2677; b) S. Bareyt, S. Piligkos, B. Hasenknopf, P. Gouzerh, E. Lacôte, S. Thorimbert, M. Malacria, *Angew. Chem.* **2003**, *115*, 3526–3528; *Angew. Chem. Int. Ed.* **2003**, *42*, 3404–3406; c) M. Sadakane, M. H. Dickman, M. T. Pope, *Inorg. Chem.* **2001**, *40*, 2715–2719; d) V. Soghomonian, Q. Chen, R. C. Haushalter, J. Zubieta, C. J. O'Connor, *Science* **1993**, *259*, 1596–1599; e) M. H. Alizadeh, K. T. Holman, M. Mirzaei, H. Razavi, *Polyhedron* **2006**, *25*, 1567–1570; f) S. T. Zheng, J. Zhang, J. Q. Xu, G. Y. Yang, *J. Solid State Chem.* **2005**, *178*, 3740–3746; g) S. T. Zheng, J. Zhang, G. Y. Yang, *J. Mol. Struct.* **2005**, *752*, 25–31.

[8] a) F. B. Xin, M. T. Pope, *J. Am. Chem. Soc.* **1996**, *118*, 7731–7736; b) M. Inoue, T. Yamase, *Bull. Chem. Soc. Jpn.* **1995**, *68*, 3055–3063; c) M. Inoue, T. Yamase, *Bull. Chem. Soc. Jpn.* **1996**, *69*, 2863–2868; d) D. L. Long, P. Kögerler, L. J. Farrugia, L. Cronin, *Chem. Asian J.* **2006**, *1*, 352–357; e) D. L. Long, E. Burkholder, L. Cronin, *Chem. Soc. Rev.* **2007**, *36*, 105–121; f) C. Streb, D. L. Long, L. Cronin, *Chem. Commun.* **2007**, 471–473; g) U. Kortz, M. G. Savelieff, F. Y. A. Ghali, L. M. Khalil, S. A. Maalouf, D. I. Sinno, *Angew. Chem.* **2002**, *114*, 4246–4249; *Angew. Chem. Int. Ed.* **2002**, *41*, 4070–4073; h) X. K. Fang, T. M. Anderson, C. L. Hill, *Angew. Chem.* **2005**, *117*, 3606–3610; *Angew. Chem. Int. Ed.* **2005**, *44*, 3540–3544; i) X. K. Fang, T. M. Anderson, Y. Hou, C. L. Hill, *Chem. Commun.* **2005**, 5044–5046.

[9] a) L. Pérez-García, D. B. Amabilino, *Chem. Soc. Rev.* **2002**, *31*, 342–356; b) L. Pérez-García, D. B. Amabilino, *Chem. Soc. Rev.* **2007**, *36*, 941–967; c) J. Jacques, A. Collet, S. H. Wilen, *Enantiomers, Racemates and Resolutions*, Krieger, Malabar, **1994**.

[10] I. Katsuki, Y. Motoda, Y. Sunatsuki, N. Matsumoto, T. Nakashima, M. Kojima, *J. Am. Chem. Soc.* **2002**, *124*, 629–640.

[11] C. P. Brock, W. B. Schweizer, J. D. Dunitz, *J. Am. Chem. Soc.* **1991**, *113*, 9811–9820.

[12] a) Y. Hou, X. K. Fang, C. L. Hill, *Chem. Eur. J.* **2007**, *13*, 9442–9447; b) Y. Q. Lan, S. L. Li, Z. M. Su, K. Z. Shao, J. F. Ma, X. L. Wang, E. B. Wang, *Chem. Commun.* **2008**, 58–60.

[13] a) A. K. Cheetham, C. N. R. Rao, R. K. Feller, *Chem. Commun.* **2006**, 4780–4795; b) N. Guillou, Q. M. Gao, P. M. Forster, J. S. Chang, S. E. Park, G. Férey, A. K. Cheetham, *Angew. Chem.* **2001**, *113*, 2913–2916; *Angew. Chem. Int. Ed.* **2001**, *40*, 2831–2834; c) P. M. Forster, A. K. Cheetham, *Angew. Chem.* **2002**, *114*, 475–477; *Angew. Chem. Int. Ed.* **2002**, *41*, 457–459; d) C. Livage, P. M. Forster, N. Guillou, M. M. Tafoya, A. K. Cheetham, G. Férey, *Angew. Chem.* **2007**, *119*, 5981–5983; *Angew. Chem. Int. Ed.* **2007**, *46*, 5877–5879; e) C. Serre, F. Millange, S. Surble, J. M. Greneche, G. Férey, *Chem. Mater.* **2004**, *16*, 2706–2711; f) C. Livage, C. Egger, G. Férey, *Chem. Mater.* **2001**, *13*, 410–414; g) S. O. H. Gutschke, D. J. Price, A. K. Powell, P. T. Wood, *Angew. Chem.* **2001**, *113*, 1974–1977; *Angew. Chem. Int. Ed.* **2001**, *40*, 1920–1923; h) Z. Wang, B. Zhang, H. Fujiwara, H. Kobayashi, M. Kurmoo, *Chem. Commun.* **2004**, 416–417; i) D. N. Dybtsev, H. Chun, S. H. Yoon, D. Kim, K. Kim, *J. Am. Chem. Soc.* **2004**, *126*, 32–33.

[14] a) C. Streb, C. Ritchie, D. L. Long, P. Kogerler, L. Cronin, *Angew. Chem.* **2007**, *119*, 7723–7726; *Angew. Chem. Int. Ed.* **2007**, *46*, 7579–7582; b) H. Q. Tan, Y. G. Li, Z. M. Zhang, C. Qin, X. L. Wang, E. B. Wang, Z. M. Su, *J. Am. Chem. Soc.* **2007**, *129*, 10066–10067.

[15] a) J. Zhang, S. M. Chen, H. Valle, M. Wong, C. Austria, M. Cruz, X. H. Bu, *J. Am. Chem. Soc.* **2007**, *129*, 14168–14169; b) G. Férey, F. Millange, M. Morcrette, C. Serre, M. L. Doublet, J. M. Greneche, J. M. Tarascon, *Angew. Chem.* **2007**, *119*, 3323–3327; *Angew. Chem. Int. Ed.* **2007**, *46*, 3259–3263; c) N. Guillou, C. Livage, M. Drillon, G. Férey, *Angew. Chem.* **2003**, *115*, 5472–5475; *Angew. Chem. Int. Ed.* **2003**, *42*, 5314–5317.

[16] a) P. C. M. Duncan, D. M. L. Goodgame, S. Menzer, D. J. Williams, *Chem. Commun.* **1996**, 2127–2128; b) J. F. Ma, J. F. Liu, Y. Xing, H. Q. Jia, Y. H. Lin, *J. Chem. Soc. Dalton Trans.* **2000**, 2403–2407; c) B. X. Dong, J. Peng, C. J. Gümez-García, S. Benmansour, H. Q. Jia, N. H. Hu, *Inorg. Chem.* **2007**, *46*, 5933–5941; d) Y. Q. Lan, S. L. Li, X. L. Wang, K. Z. Shao, Z. M. Su, E. B. Wang, *Inorg. Chem.* **2008**, *47*, 529–534;

[17] a) H. L. Ngo, W. B. Lin, *J. Am. Chem. Soc.* **2002**, *124*, 14298–14299; b) Y. Cui, S. J. Lee, W. B. Lin, *J. Am. Chem. Soc.* **2003**, *125*, 6014–6015; c) P. A. Maggard, C. L. Stern, K. R. Poeppelmeier, *J. Am. Chem. Soc.* **2001**, *123*, 7742–7743; d) B. Yan, M. D. Capracotta, P. A. Maggard, *Inorg. Chem.* ***2005****, 44*, 6509–6511; e) P. A. Maggard, A. L. Kopf, C. L. Stern, K. R. Poeppelmeier, K. M. Ok, P. S. Halasyamani, *Inorg. Chem.* **2002**, *41*, 4852–4858; f) M. C. Hong, *Cryst. Growth Des.* **2007**, *7*, 10–14; g) L. Han, M. C. Hong, R. H. Wang, J. H. Luo, Z. Z. Lin, D. Q. Yuan, *Chem. Commun.* **2003**, 2580–2581; h) J. H. Luo, Y. S. Zhao, H. G. Xu, T. L. Kinnibrugh, D. L. Yang, T. V. Timofeeva, L. L. Daemen, J. Z. Zhang, W. Bao, J. D. Thompson, R. P. Currier, *Inorg. Chem.* 2007, 46, 9021–9023; i) J. Zhang X. H. Bu, *Angew. Chem.* **2007**, *119*, 6227–6230; *Angew. Chem. Int. Ed.* **2007**, *46*, 6115–6118.

[18] a) L. M. Zheng, T. Whitfield, X. Wang, A. J. Jacobson, *Angew. Chem.* **2000**, *112*, 4702–4705; *Angew. Chem. Int. Ed.* **2000**, *39*, 4528–4531; b) G. Paul, A. Choudhury, R. Nagarajan, C. N. R. Rao, *Inorg. Chem.* **2003**, *42*, 2004–2013; c) J. R. D. DeBord, Y. Zhang, R. C. Haushalter, J. Zubieta, C. J. O'Connor, *J. Solid State Chem.* **1996**, *122*, 251–258; d) Y. Xu, G. P. Zhou, D. R. Zhu, *Inorg. Chem.* **2008**, *47*, 567–571.

[19] A. M. P. Peedikakkal, J. J. Vittal, *Cryst. Growth Des.* **2008**, *8*, 375–377.

[20] a) L. Carlucci, G. Ciani, D. M. Proserpio, *Coord. Chem. Rev.* **2003**, *246*, 247–289; b) S. R. Batten, R. Robson, *Angew. Chem.* **1998**, *110*, 1558–1595; *Angew. Chem. Int. Ed.* **1998**, *37*, 1460–1494; c) S. R. Batten, *CrystEngComm* **2001**, 67–72; d) V. A. Blatov, L. Carlucci, G. Ciani, D. M. Proserpio, *CrystEngComm* **2004**, *6*, 378–395.

[21] a) X. L. Wang, C. Qin, E. B. Wang, Z. M. Su, L. Xu, S. R. Batten, *Chem. Commun.* **2005**, 4789–4791; b) X. L. Wang, C. Qin, E. B. Wang, Z. M. Su, *Chem. Eur. J.* **2006**, *12*, 2680–2691; c) L. Carlucci, G. Ciani, D. M. Proserpio, F. Porta, *Angew. Chem.* ***2003****, 115*, 331–336; *Angew. Chem. Int. Ed.* **2003**, *42*, 317–322; d) X. Li, R. Cao, D. F. Sun, W. H. Bi, D. Q. Yuan, *Eur. J. Inorg. Chem.* **2004**, 2228–2231; e) Y. Q. Lan, S. L. Li, X. L. Wang, Z. M. Su, K. Z. Shao, E. B. Wang, *Chem. Commun.* **2007**, 4863–4865; f) J. Zhang, Y. G. Yao, X. H. Bu, *Chem. Mater.* **2007**. *19*. 5083–5089; g) X. S. Qu, L. Xu, G. G. Gao, F. Y. Li, Y. Y. Yang, *Inorg. Chem.* **2007**, *46*, 4775–4777.
[22] L. Pasteur, *Ann. Chim. Phys.* **1848**, *24*, 442–459.
[23] a) E. Q. Gao, Y. F. Yue, S. Q. Bai, Z. He, C. H. Yan, *J. Am. Chem. Soc.* **2004**, *126*, 1419–1429; b) C. He, Y. G. Zhao, D. Guo, Z. H. Lin, C. Y. Duan, *Eur. J. Inorg. Chem.* **2007**, 3451–3463; c) C. Y. Chen, P. Y. Cheng, H. H. Wu, H. M. Lee, *Inorg. Chem.* **2007**, *46*, 5691–5699.
[24] R. Ludwig, *Angew. Chem.* **2001**, *113*, 1856–1876; *Angew. Chem. Int. Ed.* **2001**, *40*, 1808–1827.
[25] a) H. Y. An, E. B. Wang, D. R. Xiao, Y. G. Li, Z. M. Su, L. Xu, *Angew. Chem.* **2006**, *118*, 918–922; *Angew. Chem. Int. Ed.* **2006**, *45*, 904–908; b) H. R. Wen, C. F. Wang, Y. Z. Li, J. L. Zuo, Y. Song, X. Z. You, *Inorg. Chem.* **2006**, *45*, 7032–7036; c) W. G. Lu, J. Z. Gu, L. Jiang, M. Y. Tan, T. B. Lu, *Cryst. Growth Des.* **2008**, *8*, 192–199.
[26] G. M. Sheldrick, SHELXS-97, Programs for X-ray Crystal Structure Solution, University of Göttingen, Göttingen, Germany, **1997**.
[27] G. M. Sheldrick, SHELXL-97, Programs for X-ray Crystal Structure Refinement, University of Göttingen, Göttingen, Germany, **1997**.
[28] L. J. Farrugia, WINGX, A Windows Program for Crystal Structure Analysis, University of Glasgow, Glasgow, UK, **1988**.

Received: April 8, 2008
Published online: September 22, 2008

